Representing socio-economic factors in the INFERNO global fire model using the Human Development Index

João C. M. Teixeira[1,2,4], Chantelle Burton[1], Douglas I. Kelley[3], Gerd A. Folberth[1], Fiona M. O'Connor[1,2], Richard A. Betts[1,2], and Apostolos Voulgarakis[4,5]

[1]Met Office, Fitzroy Road, EX1 3PB, Exeter, UK
[2]Global Systems Institute, University of Exeter, EX4 4QE, UK
[3]UK Centre for Ecology and Hydrology, Wallingford OX10 8BB, U.K
[4]Leverhulme Centre for Wildfires, Environment and Society, Department of Physics, Imperial College London, London, UK
[5]School of Environmental Engineering, Technical University of Crete, Chania, Greece

Correspondence: João C. M. Teixeira (joao.teixeira@metoffice.gov.uk)

Abstract. Humans can act as fire starters or suppressors, changing fire regimes by increasing the number of ignitions, changing their timing, and altering fuel structure and abundance, which can be considered a human–environmental coupling. Considering the human influences on fire activity, representing socio-economic impacts on fires in global fire models is crucial to underpin the confidence in these modelling frameworks. In this work we implement a socio-economic factor in the fire ignition and suppression parametrisation in INFERNO based on a Human Development Index (HDI). HDI captures human development's income, health, and education dimensions leading to a representation where if there is more effort to improve human development, the population also invests in higher fire suppression. Including this representation of socio-economic factors in INFERNO reduces the annual mean burnt area (between 1997 - 2016) positive biases found in Temperate North America, Central America, Europe and Southern Hemisphere South America, by more than 100 % without statistically significant impact to other areas. In addition, it improves the representation of the burnt area trends, especially in Africa. Central Asia and Australia where observations show negative trends. Including socio-economic impacts on fire based on HDI in INFERNO provides a simple and linear representation of these effects on fire ignition and suppression, leading to an improvement of the model performance, especially in developed regions, These impacts are especially relevant to understand future climate regimes and inform policymakers on effects of fire policy in a changing climate.

1 Introduction

Fire is a global-scale environmental process and a critical Earth System component that influences climate, atmospheric composition, vegetation, biogeochemical cycles and human activities (Bowman et al., 2009; Daniau et al., 2013; Solomon et al., 2022). Humans can act as fire starters or suppressors, changing fire regimes by increasing the number of ignitions, changing their timing and altering fuel structure and abundance, which can be considered a human–environmental coupling (Marlon et al., 2008; Archibald et al., 2009; Bowman et al., 2011; Andela and Van Der Werf, 2014), thereby changing background levels of natural fire activity. Different cultural and political influences in fire management can shape fire regimes at a regional

level (Bowman et al., 2011; Chinamatira et al., 2016; Sullivan et al., 2022). For example, governments may allow the logging of burnt forests, adding incentive to setting forests alight. Moreover, in flammable biomes, such as tropical savannas and seasonally dry forests, maintained by their natural fire regimes, policies to reduce fire risk to humans and their infrastructure or

25   support their livelihoods may change the fire regimes and the biodiversity they support (Laris, 2002). However, this can be greatly affected by a lack of public support and resources, inadequate training, ambiguous laws, and lack of deterrent measures (Chinamatira et al., 2016).

   Studies from Riley et al. (2019) and Andela et al. (2017) provide an overview of the impacts of climate, fuel availability and human drivers on fires globally and throughout different regions. These studies highlight that a reduction of global burned

30   area is driven by a decline of 1.27% per year in Africa that is likely the result of human-mediated landscape changes (Andela et al., 2017), suggesting that, for this region, human impacts on fire activity are dominant over the global climate feedback which would increase fire activity globally. Furthermore, Andela et al. (2017) demonstrates that human population density and prosperity can significantly impact burnt areas. On the one hand, areas with low population density are associated with lower burnt areas, and densely populated areas tend to be associated with increased burnt area. On the other hand, for heavily

35   populated and prosperous regions, burnt area decline is likely a function of perceived threats to highly valued infrastructure, prompting extensive fire suppression efforts, sometimes involving high monetary costs.

   Most fire models follow a representation of anthropogenic fire ignitions where there is an increase of fire ignitions with increasing population density up to a point at which human suppression becomes the dominant factor and fire ignitions are reduced as the population rises (Rabin et al., 2017; Teckentrup et al., 2019). This approach does not account for the socio-

40   economic impacts of anthropogenic fire ignitions or suppression. It does not capture how humans influence regional variation in contemporary burning practices. Ford et al. (2021) reviewed different approaches to modelling human-fire interactions from different disciplinary contexts. In their work, the authors have noted that global fire models often apply simplistic representations of human ignitions, generally specified as a function of population density, increasing up to a threshold value after which there are no additional ignitions with an increasing population. Although some models represent ignitions depending on

45   human economic activities (e.g., Pfeiffer et al. (2013)), creating appropriate driving data sets is vital to implement human-fire interactions in global models realistically.

   Chuvieco et al. (2021) analysed burnt area trends, as well as interannual variability at regional and global scales, focusing on human control of fires. In this study, the authors show that one of the human variables that were more clearly associated with fire variability was the Human Development Index (HDI). In addition, it also demonstrated that burnt areas tend to be

50   similar in different years when HDI values decrease and when cropland and livestock density increase, probably due to using agricultural practices less dependent on fire. Furthermore, the work of Li et al. (2013) includes an implementation of socio-economic impacts of fire, based on the use of the Gross domestic product, to parametrise the anthropogenic influences on fires. However, this is only applied to agricultural fires, not accounting for human factors in managing fires holistically.

   In addition Bowman et al. (2020) showed that human influences on fire activity have become more pronounced since the

55   late eighteenth century; this is due to the effects of reflecting the effects of industrialisation and climate change, land clearance, human population growth, replacement of indigenous and traditional fire management, and the subsequent development of

large-scale firefighting and fuel management in the twentieth century. Considering this, there is a need for data collection to improve the quantification and modelling of fire activity and human populations, including their socio-economic status and historical and cultural and political legacies especially as vegetation fires' economic and environmental impacts will worsen

60   due to anthropogenic climate change (Kelley et al., 2019). Furthermore, Nikolakis and Roberts (2022) explored how policy learning can occur within wildfire governance and how wildfire policies have evolved in British Columbia. This case study demonstrates that policy transfer from similar contexts, Indigenous peoples and their governments, can reframe perceptions of wildfire risk and solutions as we learn to live with wildfire in an increasingly uncertain future. In addition, several authors have shown that for developed regions, land and fire management policies on the land and fire management have a greater role

65   than other human behaviours in controlling ignitions (Nikolakis and Roberts, 2022; Jacobson et al., 2022; Ford et al., 2021; Carreiras et al., 2014; Mourão and Martinho, 2014).

Socio-economic and adaptation policies have a large impact on fire regimes in an evolving climate. Therefore, representing these in global fire models is crucial to build confidence in the modelling frameworks which are used to understand future climate regimes. This, in turn, can underpin decision-making by policy-makers in regards to fire policy in the future.

70   In this work, we explore the use of the HDI to represent socio-economic impacts on fires in the Pechony and Shindell (2009) anthropogenic fire ignitions representation, building on the work of Mangeon et al. (2016), to represent socio-economic impacts on fires. We aim to improve the regional representation of human–environmental coupling for applications at large spatial scales within an Earth System Model (ESM) context.

Section 2 describes the INFERNO fire model, the coupling of INFERNO to the latest representation of the land surface

75   model (JULES-ES) as used in the UK's Earth System Model (UKESM1), and how we include HDI into INFERNO's ignition scheme. In Section 3, we evaluate the impact of considering HDI on burnt area, burnt area trends, as well as the impact of external model drivers of burnt area trends. Discussion and conclusions from this work are presented in Section 4 where we focus on novel model results, placing the link between socio-economic factors and fires in context with existing literatureModel limitations and known issues are also highlighted..

2   Methods

2.1   INFERNO fire model

We simulate fire using the INFERNO (INteractive Fires and Emissions algoRithm for Natural envirOnments; Mangeon et al. (2016)) fire model. INFERNO uses an approach based on Pechony and Shindell (2009), adapted to allow interaction within an ESM framework. More precisely, INFERNO uses water vapour pressure deficit as one of the main indicators of flammability

85   and an inverse exponential relationship to relate flammability to soil moisture.

The burnt area, represented in Eq. 1, is associated with an average burnt area per fire for each model plant functional type (PFT). This decouples the fire spread stage from local meteorology and topography, processes not typically resolved in coarse grids, such as those often used within ESMs.

Biogeosciences
Discussions

$$BA_{PFT} = I_T \, F_{PFT} \, \overline{BA_{PFT}} \tag{1}$$

where I_T represents the fire ignitions, including natural and human ignitions as well as fire suppression by humans, F_{PFT} the flammability per PFT dependent on the 1.5 m temperature, 1.5 m relative humidity and fuel density - as defined in Eq. 4 through 6 from Mangeon et al. (2016) - and $\overline{BA_{PFT}}$ is the average burnt area for each PFT.

INFERNO fire ignitions are split into Natural Ignitions (I_N) from cloud to ground lightning flashes and from Human activities (I_A) dependent on population density (PD) as described in Eq. 2. Humans are also responsible for suppressing fires in the model, using a suppression function (f_{NS}) dependent on human population density (Eq. 3). The total ignitions (I_T) are represented by Eq. 4.

$$I_A = k_{(PD)} \, PD\alpha \times (\textbf{1 - HDI}) \tag{2}$$

$$f_{NS} = 7.7 \left(0.05 + 0.9 \times e^{-0.05 \, PD}\right) \times (\textbf{1 - HDI}) \tag{3}$$

$$I_T = (I_N + I_A)\frac{f_{NS}}{8.64 \times 10^{10}} \tag{4}$$

where $k_{(PD)} = 6.8 \times PD - 0.6$ is a function that represents the varying anthropogenic influence on ignitions in rural versus urban environments, and the parameter $\alpha = 0.03$ represents the number of potential ignition sources per person per month per km^2, and HDI represents the Human Development Index.

Previously, INFERNO only included information on population density. To represent the socio-economic factors impacting fire ignition and suppression, we include a Human Development Index (HDI) term $(1 - HDI)$ in our human ignition and suppression Eq. 2 and 3 (shown in bold).

HDI provides a single index measure, calculated based on four key metrics (Bhanojirao, 1991):

- life expectancy at birth

- expected years of schooling

- average years of schooling

- gross national income (GNI) per capita

These metrics are then normalised by their respective maximum value, and HDI is calculated as the geometric mean of life expectancy, education, and GNI per capita, as shown in Eq. 5

Biogeosciences
Discussions

$$HDI = (H_N \cdot E_N \cdot I_N)^{\frac{1}{3}}$$ (5)

where H_N is the normalised life expectancy, E_N is the normalised arithmetic mean of the two education indices and I_N is
115   the normalised GNI.

In this representation of socio-economic impacts on fire ignition and suppression, we assume that fire ignitions decrease and
fire suppression increases for areas with more effort in human development improvements. Moreover, it reduces the impact
changes in population density have in areas with high HDI while keeping a dependency on population density changes for areas
with low HDI, where policies on land and fire management have a greater role than other human behaviours in controlling
120   ignitions (Nikolakis and Roberts, 2022; Ford et al., 2021; Jacobson et al., 2022; Carreiras et al., 2014; Mourão and Martinho,
2014). The impact of HDI on INFERNO anthropogenic fire ignitions, represented as I_A (Eq. 2), is depicted in Figure 1.
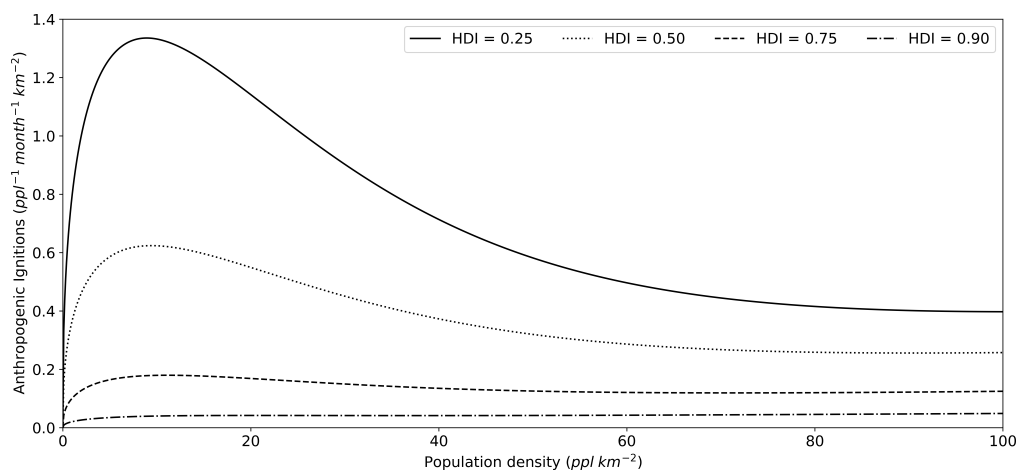

Figure 1. Anthropogenic fire ignitions ($ppl^{-1}\ month^{-1}\ km^{-2}$) as a function of population density ($ppl\ km^{-2}$) and Human Development
Index.

We obtained HDI data from the gridded global datasets for Gross Domestic Product and Human Development Index (Kummu
et al., 2018), which provides HDI data from 1979 to 2020. To cover the full modelled period (1860-2016), the HDI data is
linearly ramped from the minimum HDI value of the dataset (0.2) to its value in 1979 for each grid point. The anthropogenic
125   ignitions term (I_A) is represented by Eq. 2, the fraction of fires not suppressed by humans (f_{NS}) by Eq. 3 and the total ignitions
(I_T) are represented by Eq. 4.

2.2 JULES-ES and INFERNO

We use the community land surface model JULES (Joint UK Land Environment Simulator; Clark et al. (2011); Best et al.
(2011)) at version 5.7, with the science configuration of the land surface as used in UKESM1 (Sellar et al., 2019), including 13
130   PFTs, and dynamic vegetation from TRIFFID (Top-down Representation of Interactive Foliage and Flora Including Dynamics;

Cox et al. (2000); Cox (2001)). This configuration of JULES is known as JULES-ES (Mathison et al., 2022). JULES simulates surface fluxes of water, energy, vegetation and carbon. Here, we use JULES as a stand-alone offline model run at a spatial resolution of N96 (equivalent to a horizontal resolution of 135 km in the mid-latitudes). The Climate Research Unit - National Centers for Environmental Predictions reanalysis (CRU-NCEP v7) (Harris et al., 2014; Viovy, 2018) atmospheric variables are

135 provided at 6-hourly intervals to drive JULES, including CO_2, precipitation, temperature, specific humidity, wind, air pressure, and short and long wave radiation. The model runs from 1860–2016 with this forcing. In this work, we analyse the period that overlaps with observations (1997-2016).

We use the latest fire-vegetation coupling described in Burton et al. (2019a) and Burton et al. (2020), incorporating additional feedbacks to the carbon cycle from litter and vegetation burning. This setup includes mortality due to fire by plant functional

140 type (PFT), which is set to 40 % for trees, 60 % for shrubs, and 100 % for grasses. This setup differs from that used in Teixeira et al. (2021), where no fire-vegetation feedbacks were considered.

Fire ignitions are based on population density data from HYDE 3.2 (Klein Goldewijk et al., 2017); (Goldewijk et al., 2017) and monthly lightning flashes climatology from LIS-OTD (Lightning Imaging Sensor – Optical Transient Detector; Cecil (2006)) observations over 1995-2014, regridded from 0.5-degree resolution to N96 (1.25 degree latitude × 1.875 degree

145 longitude). After spinning up the model to equilibrium, we complete a full historical simulation from 1860-2019 at N96 and use results from the present day (1997-2015) for our analysis to compare with available observations of burnt area.

We performed two model experiments to test the impact of representing the socio-economic factors on fire ignition and suppression in INFERNO. A control experiment referred to as JULES-INFERNO, and a similar experiment, including socio-economic factors on fire ignition and suppression parametrisation described in section 2.1, referred as to JULES-INFERNO+HDI.

150 Introducing the socio-economic factors in JULES-INFERNO+HDI significantly reduced global burnt area, leading to a large negative bias compared to observations (not shown). This is because the model has until now been tuned to observations excluding socio-economic factors, introducing compensating errors, especially in the average burnt area by PFT, which is generally defined heuristically. To address this, we have revised the values used for $\overline{BA_{PFT}}$ in line with the latest available literature from Andela et al. (2019), adapted for the JULES PFTs. In the JULES-INFERNO+HDI experiment, we use the

155 revised $\overline{BA_{PFT}}$ values. The $\overline{BA_{PFT}}$ values in both experiments are detailed in table 1.

2.3 Burnt area evaluation

We use data from the Global Fire Emission Database version 4 (GFED4s) (Giglio et al., 2013) to assess the model performance in simulating burnt area. This dataset is provided as a gridded product at a $0.25°$ resolution. It is derived from a multi-sensor satellite dataset, including satellite data based on active fire detection, and including small fires based on statistical modelling,

160 as detailed in (Randerson et al., 2012). We apply regions defined in the GFED4s dataset to the modelled data to evaluate the results at a regional level (Figure 2).

When comparing datasets (modelled or observed) at different grid resolutions, the higher-resolution dataset is re-gridded to the lowest-resolution grid using a first-order conservative area-weighted re-gridding method.
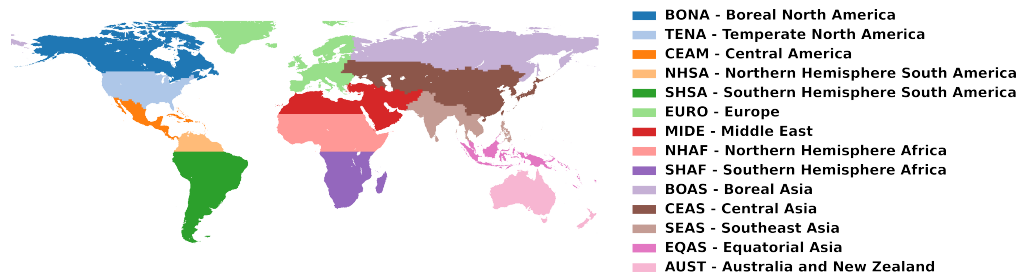
Figure 2. Basis regions, as defined in the GFED4s dataset (Giglio et al., 2013).

Table 1. Biomass burning average burnt areas ($km^2\ fire^{-1}$) for various plant functional types based on Burton et al. (2019a) (top row) and adapted from Andela et al. (2019) (bottom row).

	Broadleaf tree			Needleleaf tree		C3			C4			Shrubs	
	Deciduous	Evergreen		Evergreen	Deciduous	Grass	Crop	Pasture	Grass	Crop	Pasture	Deciduous	Evergreen
		Tropical	Temperate										
$\overline{BA_{PFT}}$	1.7	1.7	1.7	1.7	1.7	3.2	0.4	3.2	3.2	0.4	3.2	2.7	2.7
Revised $\overline{BA_{PFT}}$	5.2	1.4	2.5	5.2	5.2	10.2	1.4	1.4	10.2	1.4	1.4	5.1	5.1

3 Results

3.1 Evaluation of burnt area

To better understand the regional impact of implementing the socio-economic factors on fire ignition and suppression in IN-FERNO, we focus on the burnt area results averaged over the GFED4s regions as defined in Figure 2.

Both model experiments reproduce the overall geographical pattern of the annual average burnt area fraction (Figure 3), though with some regional differences compared to observations. For instance, JULES-INFERNO simulates the observed pattern in the major fire regions: South America, Africa and Eurasia. However, it shows substantial spatial biases over North America, Europe and Asia, leading to a low global spatial correlation of 26.5 % compared with GFED4s. Conversely, JULES-INFERNO+HDI, reduces fires in the regions with higher HDI values, reducing the biases seen in JULES-INFERNO and resulting in a better agreement with GFED4s. This experiment has a global pattern correlation of 46.5 % when compared with GFED4s.

Including a parametrisation for socio-economic factors on fire ignition and suppression reduces the burnt area in regions with high prosperity (high values of HDI), leading to improvements over North America, Europe and Asia, as shown in Figure 4. Moreover, compared to JULES-INFERNO, JULES-INFERNO+HDI reduces the positive bias over South America and India, although it increases the negative bias over the boreal regions, Australia, and South East Asia.

JULES-INFERNO+HDI has a smaller bias than JULES-INFERNO globally, except for savanna regions in Africa, Australia, and central Eurasia.
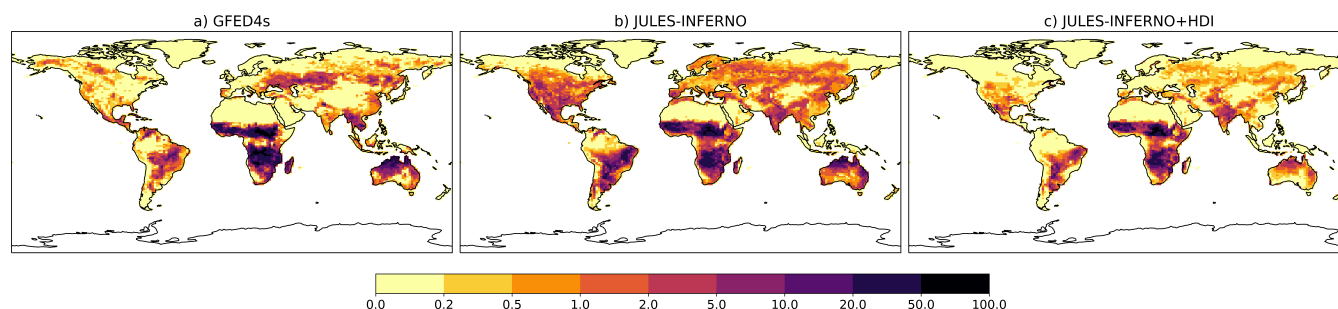
7

Figure 3. Burnt area fraction (%) mean annual average (1997 - 2016) for a) GFED4s, b) JULES-INFERNO and c) JULES-INFERNO+HDI.
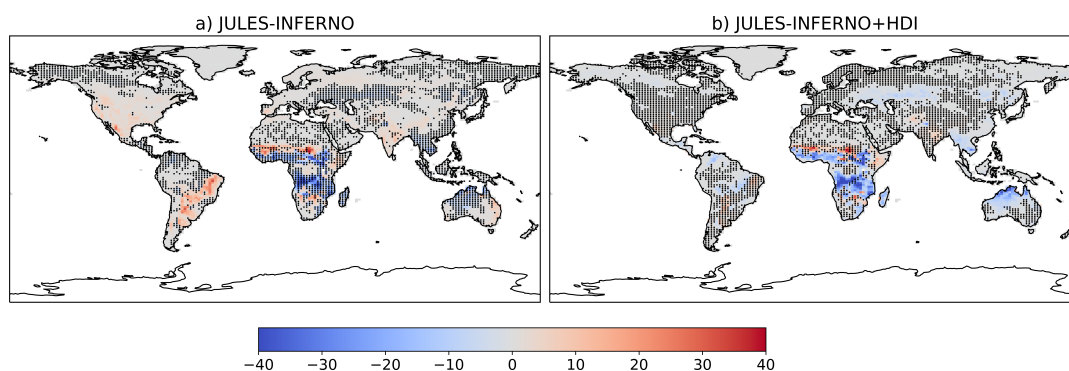

Figure 4. Burnt area fraction (%) mean annual average bias (1997 - 2016) for a) JULES-INFERNO and b) JULES-INFERNO+HDI. Stippling shows the points where the bias is smaller than in its counterpart experiment.

Figure 5 shows the burnt area annual mean time series. In addition, and to aid the analysis of these time series, we performed statistical analysis including various metrics such as, the Root Mean Squared Error (RMSE), Root Mean Squared Error after removal of constant mean bias (RMSE$_{UE}$), the bias, Pearson correlation, and Standard Deviation (STD) of the burnt area monthly and annual mean time series for all GFED4s regions (Table 2). We also assess the model's ability to reproduce
185 observed trends using a simple log-transformed linear regression. For conciseness, this analysis focuses on the regions with the largest change between the JULES-INFERNO and JULES-INFERNO+HDI experiments. Nonetheless, an additioanl figure containing the results for all GFED4s regions is provided as supplementary material in Figure A1.

To analyse the model performance, we calculated the following statistical and error measures, relative to observations:

- Deviation of the modelled data in relation to observed values:

190
$$\phi'_i = \phi_i - \phi_{i,obs} \tag{6}$$

- Bias, which represents the mean deviation of the modelled data in relation to the observed values.

$$Bias = \frac{1}{N}\sum_{i=1}^{N}\phi'_i \tag{7}$$

Biogeosciences
Discussions

Open Access

EGU

– The Root Mean Square Error.

$$RMSE = \sqrt{\frac{\sum\limits_{i=1}^{N} \left(\phi_i - \phi_{i,obs}\right)^2}{N}} \tag{8}$$

195   – The Root Mean Square Error after the removal of a constant bias.

$$RMSE_{UB} = \sqrt{\frac{\sum\limits_{i=1}^{n} \left[\left(\phi_i - \overline{\phi}\right) - \left(\phi_{i,obs} - \overline{\phi_{obs}}\right)\right]^2}{N}} \tag{9}$$

– Standard deviation for the modelled - equation 10 - and observed - equation 11 - data.

$$S = \sqrt{\frac{\sum\limits_{i=1}^{n} \left(\phi_i - \overline{\phi}\right)^2}{N}} \tag{10}$$

$$S_{obs} = \sqrt{\frac{\sum\limits_{i=1}^{n} \left(\phi_{i,obs} - \overline{\phi_{obs}}\right)^2}{N}} \tag{11}$$

200   were i is the temporal index and N is the number of elements of ϕ considered.

Considering the statistics presented in Table 2, a perfect simulation would have the following criteria:

– RMSE = 0

– RMSE$_{UE}$ = 0

205   – bias = 0

– Pearson correlation = 100 %

– STD / STD$_{GFED4s}$ = 1

– RMSE / STD$_{GFED4s}$ = 0

– RMSE$_{UE}$ / STD$_{GFED4s}$ = 0

210   The results presented both in Figure 5 and Table 2 show that the inclusion of the socio-economic factors in INFERNO leads to improvements in the simulation of annual burnt area for regions such as Temperate North America (TENA), Central America (CEAM), Southern Hemisphere South America (SHSA), Europe (EURO), consequently reducing the large relative

Biogeosciences
Discussions
Open Access
EGU

Table 2. Annual burnt area statistics for the different GFED4s fire regions (Giglio et al., 2013).

| Group	Statistic	GLOBAL	BONA	TENA	CEAM	NHSA	SHSA	EURO	MIDE	NHAF	SHAF	BOAS	CEAS	SEAS	EQAS	AUST
GFED4s	Mean BA (Mha)	476.43	2.47	2.33	1.68	4.94	25.85	0.86	0.90	152.24	155.85	7.65	19.22	12.85	0.70	39.88
	Trend (Mha year^{-1})	-6.77	0.05	0.05	-0.04	-0.05	-0.44	-0.03	0.02	-2.20	-0.54	-0.03	-0.37	0.18	-0.02	-1.09
JULES-INFERNO	Mean BA (Mha)	442.08	4.09	19.53	6.08	1.97	75.09	3.09	4.78	136.30	85.29	10.21	14.88	13.89	0.11	31.43
	Trend (Mha year^{-1})	-2.24	-0.02	0.09	0.00	0.02	-0.13	0.01	-0.04	-1.26	-0.14	0.05	0.10	0.08	0.00	0.02
	Bias (Mha)	-34.35	1.62	17.21	4.40	-2.97	49.24	2.23	3.88	-15.94	-70.56	2.56	-4.34	1.03	-0.59	-8.46
	Relative bias (%)	-7.21	65.27	739.79	262.03	-60.16	190.48	258.82	432.09	-10.47	-45.27	33.48	-22.58	8.05	-84.81	-21.20
	RMSE	47.28	2.10	17.38	4.52	3.07	49.85	2.27	3.92	20.23	71.17	4.26	7.16	1.91	0.89	21.60
	RMSE$_{UE}$	32.50	1.35	2.43	1.00	0.77	7.78	0.45	0.55	12.45	9.31	3.40	5.69	1.60	0.66	19.87
	Correlation (%)	75.25	0.22	81.58	54.76	58.26	47.88	15.35	-26.02	77.73	46.76	26.75	13.83	68.84	79.84	8.70
	STD / STD$_{GFED4s}$	0.39	0.25	4.47	0.84	0.69	0.77	0.68	1.00	0.75	0.44	0.23	0.22	0.54	0.10	0.18
	RMSE / STD$_{GFED4s}$	1.10	1.61	26.45	3.99	3.25	5.93	5.72	11.31	1.02	6.76	1.21	1.25	0.88	1.23	1.09
	RMSE$_{UE}$ / STD$_{GFED4s}$	0.75	1.03	3.70	0.89	0.82	0.93	1.12	1.59	0.63	0.88	0.96	0.99	0.74	0.92	1.00
JULES-INFERNO+HDI	Mean BA (Mha)	278.90	0.52	3.40	2.13	0.29	25.58	0.45	3.09	125.08	69.65	3.43	6.50	9.56	0.03	7.14
	Trend (Mha year^{-1})	-7.58	-0.02	-0.07	-0.05	-0.01	-0.64	-0.01	-0.11	-2.71	-1.94	-0.09	-0.22	-0.19	0.00	-0.20
	Bias (Mha)	-197.52	-1.95	1.07	0.45	-4.65	-0.27	-0.41	2.19	-27.16	-86.20	-4.22	-12.72	-3.30	-0.67	-32.74
	Relative bias (%)	-41.46	-78.97	46.08	26.56	-94.14	-1.05	-48.14	244.36	-17.84	-55.31	-55.17	-66.19	-25.64	-95.88	-82.09
	RMSE	198.99	2.37	1.34	1.03	4.73	7.87	0.53	2.35	29.19	87.11	5.44	13.80	4.23	0.97	38.14
	RMSE$_{UE}$	24.12	1.34	0.81	0.92	0.89	7.87	0.33	0.84	10.70	12.60	3.44	5.36	2.66	0.70	19.57
	Correlation (%)	84.19	-14.08	39.06	61.37	64.10	37.74	73.22	-24.81	86.33	39.02	23.13	37.02	-6.63	85.02	21.62
	STD / STD$_{GFED4s}$	0.99	0.11	1.21	0.41	0.10	0.51	0.24	1.98	1.06	1.15	0.18	0.25	0.65	0.03	0.09
	RMSE / STD$_{GFED4s}$	4.61	1.81	2.04	0.91	5.01	0.94	1.34	6.78	1.48	8.27	1.54	2.41	1.95	1.35	1.92
	RMSE$_{UE}$ / STD$_{GFED4s}$	0.56	1.02	1.23	0.82	0.94	0.94	0.84	2.43	0.54	1.20	0.97	0.94	1.23	0.97	0.99
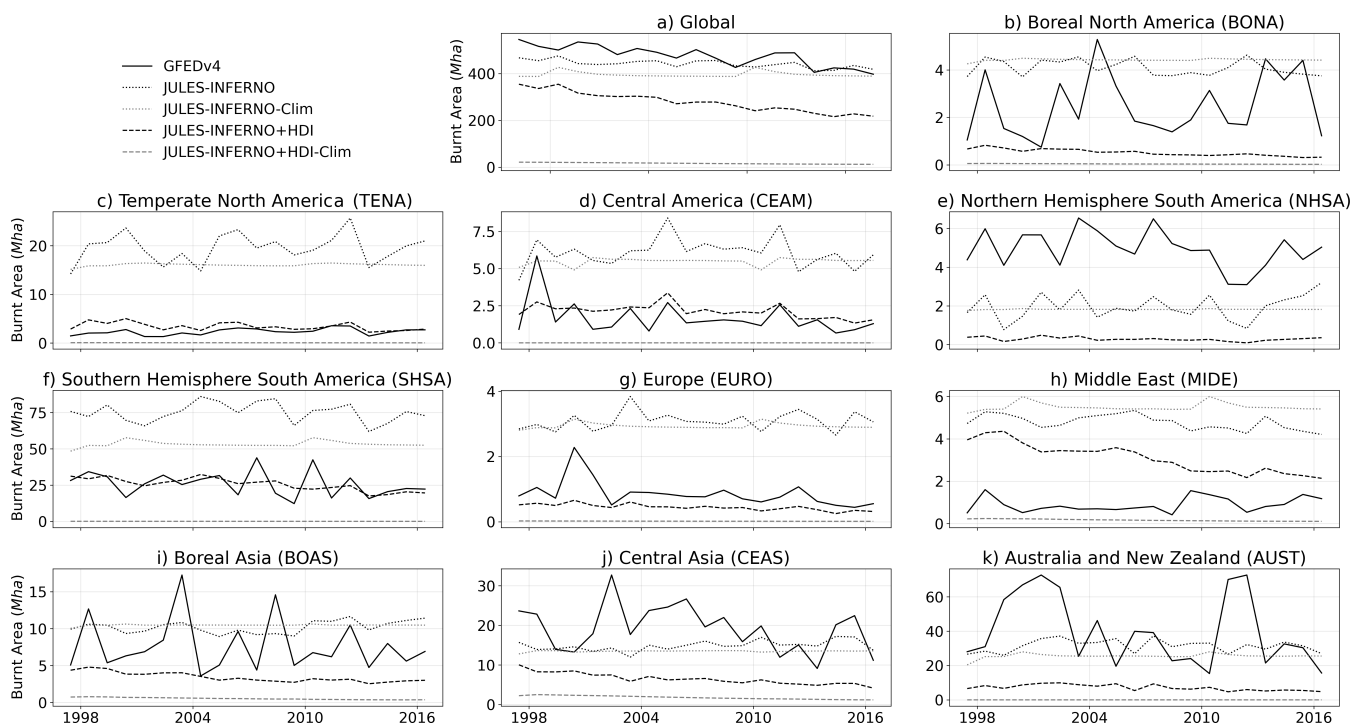
Figure 5. Burnt area annual mean time series (Mha) for the regions with the largest changes between experiments.

bias found in these regions in the JULES-INFERNO experiments. This bias reduction is especially significant for many areas with substantially large relative bias (bias greater than 150 %) in JULES-INFERNO against observations.

215   For example, the bias in the TENA region is reduced from 735.6 % in JULES-INFERNO to 44.5 % in JULES-INFERNO-HDI. Other bias reductions include 259.22 % to 24.24 % in CEAM, 191.73 % to -1.72 % in SHSA, 258.81 % to -48.79 % in EURO, and 420.52 % to 231.75 % in MIDE.

Conversely, there is an increase in the relative bias for NHSA from -60.06 % in JULES-INFERNO to -94.27 % in JULES-INFERNO+HDI and AUST from -21.79 % to -82.29 %.

220   Despite the socio-economic factors in INFERNO resulting in a reduction of bias and RMSE in regions where improvements are most needed, it also results in a general reduction in the interannual variability of the burnt area. Although this effect benefits some regions, such as TENA and CEAM, it tends to impact regions which experience high levels of burning negatively.

These results suggest that, although there is good agreement between the observed mean burnt area and JULES-INFERNO at a global scale (e.g., a bias of -7.21 %), this is due to compensating biases at the regional scale. We find that JULES-

225   INFERNO+HDI performs better regionally, improving the representation of burnt area variability (STD / STDGFED4s = 0.99; Table 2), reducing the RMSE (RMSE$_{UE}$ is reduced from 32.50 in JULES-INFERNO to 24.12 in JULES-INFERNO+HDI), and better correlating with GFED4s (correlation of 75.25 % and 84.19 % for JULES-INFERNO and JULES-INFERNO+HDI respectively; Table 2).

3.2 Impact on burnt area trends

230 Including socio-economic factors in INFERNO adds a new external forcing to the model. Through this, historical changes to socio-economic factors, represented through HDI, impact how population density changes affect fire ignitions in the model (see Section 2.1 and Figure 1). Specifically, for regions with high HDI, variations in population have less of an impact on anthropogenic ignitions, while for regions with low HDI, variations in population can have a more considerable impact. This alters the importance of population density changes for highly developed regions, making HDI the dominant factor driving
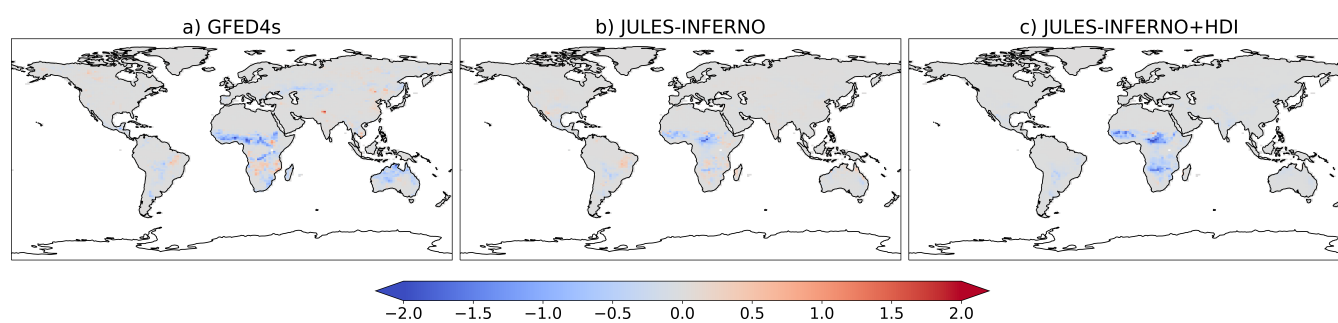
235 burnt area trends.

Figure 6. Burnt area fraction trend ($\% \, year^{-1}$) (calculated between the period 1997 - 2016) for a) GFED4s, b) JULES-INFERNO and c) JULES-INFERNO+HDI.

In figure 6, both JULES-INFERNO and JULES-INFERNO+HDI represent the main global burnt area trends. JULES-INFERNO can represent both regions with burnt area increases (e.g., Southern Africa and Northeast South America) and captures the dominant region for decreased burnt area - North Africa. However, this model setup tends to have weaker negative trends when compared to GFED4s. Conversely, JULES-INFERNO+HDI presents stronger trends, better representing those found in observations. However, it cannot reproduce the positive trends in Southern Africa and Northeast South America. JULES-INFERNO and JULES-INFERNO+HDI cannot represent the observed trends in Central Asia or Boreal North America.

Overall, including socio-economic factors in INFERNO results in an improvement in burnt area trends in comparison with observations. As seen in Table 2, JULES-INFERNO+HDI better represents the global negative trend in burnt area when compared to observations (-6.77 $Mha \, year^{-1}$ for GFED4s, -2.24 $Mha \, year^{-1}$ for JULES-INFERNO, and -7.58 $Mha \, year^{-1}$ for JULES-INFERNO+HDI). This improvement comes mostly from a better representation of the burnt area trends in regions with strong negative trends, such as SHSA, NHAF, CEAS and AUST, but also by better-representing regions with weak negative burnt area trends, namely CEAM, NHSA, EURO and BOAS. Moreover, in regions CEAM, NHSA, EURO, BOAS, CEAS, and AUST, JULES-INFERNO+HDI shows a negative burnt area trend, better agreeing with observations.

250 Contrary to these improvements, JULES-INFERNO+HDI can also produce trends that are too strong. For example, for South Hemisphere Africa (SHAF), although JULES-INFERNO+HDI has the same burnt area trend sign as in the observations (negative), the trend is too strong (-0.54 $Mha \, year^{-1}$ for GFED4s, -0.14 $Mha \, year^{-1}$ for JULES-INFERNO, and -1.94

$Mha\ year^{-1}$ for JULES-INFERNO+HDI), and JULES-INFERNO provides a better representation in these regions. In addition, for regions where observations show a positive burnt area trend (TENA, MIDE and SEAS), JULES-INFERNO+HDI has

255 a trend of opposite sign (negative). At the same time, JULES-INFERNO can capture the positive trend in TENA and SEAS.

3.2.1 Impact of external model drivers on burnt area trends

As described in section the 2.2, JULES-ES experimental setup relies on ancillary forcing data to represent external processes to JULES, such as atmospheric weather conditions, atmospheric composition, and population density, and biogenic drivers. These external forcings can drive fire by forcing changes to the evolution of land surface properties, fire ignitions, and fire

260 weather. It is important to understand the impact these external drivers have on the burnt area trends and the interaction with the parametrised socio-economic factors in fires. Therefore a set of sensitivity experiments were performed by fixing the external model drivers to the year 1990 and only allowing a given external driver to vary transiently through the experiment.

- **1990 control:** where all external model drivers are fixed to the year 1990

- **clim:** where only the atmospheric drivers are transient (downward long wave radiation flux, downward short wave
265   radiation flux, precipitation, surface pressure, air temperature, meridional and zonal Wind components)

- **tas:** where only air temperature at 2 m is transient

- **ppn:** where only precipitation is transient

- **lu:** where only the land use is transient

- **Ndep:** where only Nitrogen deposition is transient

270 - **pop:** where only population density is transient

- **CO$_2$**: where only atmospheric Carbon Dioxide mixing ratio is transient

- **HDI:** where only the Human Development Index is transient (only for JULES-INFERNO+HDI)

These sensitivity experiments branched from their respective reference runs (**ref**) - JULES-INFERNO and JULES-INFERNO+HDI - starting from 1990 and run up to 2016. In this way, the underlying land surface state from the reference run is preserved, and

275 only changes to the forcing that take place during the period of interest are taken into effect. The trends for each relevant external forcing are in Supplementary Figure A2.

The results of these sensitivity experiments on the burnt area trends ($Mha\ year^{-1}$) for the different GFED4s fire regions are presented in Table 3. Burnt area trends in JULES-INFERNO tend to be driven by climate, land use, or population density changes (relative contribution greater than 50 % when compared to their reference), with the dominant driver for the majority

280 of regions being climate (including through air temperature and precipitation), for example, BONA, TENA, NHSA, SHSA, EURO, MIDE, SHAF, BOAS, CEAS, SEAS, and AUST. On the one hand, air temperature is a significant driver of increasing

Table 3. Burnt area trends ($Mha\ year^{-1}$) for the different GFED4s fire regions (Giglio et al., 2013) from the model sensitivity experiments. Values in bold represent trends that are significantly different from zero at the 99% confidence level.

Model		GFED4s	GLOBAL	BONA	TENA	CEAM	NHSA	SHSA	EURO	MIDE	NHAF	SHAF	BOAS	CEAS	SEAS	EQAS	AUST
		GFED4s	**-6.77**	0.05	**0.05**	-0.04	-0.05	-0.44	**-0.029**	0.02	**-2.20**	-0.54	-0.03	-0.37	**0.18**	-0.02	-1.09
JULES-INFERNO	control		**-2.24**	-0.0162	0.092	0.003	0.023	-0.133	0.008	**-0.036**	**-1.263**	-0.136	0.051	**0.095**	0.078	-0.002	0.017
	1990 control		0.01	0.0015	**0.012**	0.001	-0.001	0.031	0.0002	**0.015**	0.112	**0.214**	**0.007**	**0.021**	**0.021**	**0.0006**	0.060
	clim		-0.06	**-0.0232**	0.047	0.034	0.023	0.136	-0.0012	**-0.023**	0.246	0.288	0.033	0.077	0.067	-0.0015	-0.041
	tas		0.42	0.0080	**0.082**	**0.035**	**0.015**	**0.274**	**0.0135**	0.007	0.147	0.158	**0.056**	**0.052**	0.031	0.0003	**0.125**
	ppn		**-0.92**	**-0.0070**	-0.049	0.019	0.014	-0.178	-0.0058	-0.038	-0.005	0.152	**0.034**	0.029	0.056	-0.0011	-0.117
	lu		**-0.68**	**0.0026**	**0.063**	0.005	**0.003**	**-0.155**	**0.0116**	**0.015**	**-0.278**	0.064	**0.019**	**0.030**	0.002	0.0000	0.060
	Ndep		-0.01	0.0018	0.005	0.004	-0.001	0.031	0.0001	**0.010**	0.112	**0.209**	**0.008**	**0.018**	**0.021**	**0.0006**	0.056
	pop		**-1.18**	**0.0043**	-0.026	**-0.018**	**-0.003**	-0.012	**-0.0056**	**-0.030**	**-0.480**	-0.140	**-0.009**	**0.017**	**0.044**	0.0000	0.072
	CO2		**-0.10**	**0.0028**	**0.035**	0.003	**-0.009**	-0.033	**0.0034**	**0.026**	**0.137**	0.064	**0.012**	**0.041**	**0.019**	**0.0004**	**0.094**
	control		**-7.58**	**-0.0230**	**-0.067**	**-0.048**	-0.007	**-0.645**	**-0.014**	**-0.114**	**-2.713**	**-1.939**	**-0.093**	**-0.223**	**-0.193**	-0.001	**-0.197**
JULES-INFERNO+HDI	1990 control		**-0.55**	**-0.0021**	**-0.002**	**0.000**	0.000	**-0.002**	**-0.0007**	**-0.008**	**-0.184**	**-0.198**	**-0.024**	**-0.075**	**-0.006**	0.0000	**0.000**
	clim		0.24	-0.0058	0.004	0.022	0.005	0.105	-0.0002	-0.004	0.637	0.304	**0.023**	0.037	**0.078**	-0.0005	0.024
	tas		**0.58**	**0.0024**	**0.017**	0.006	0.004	**0.139**	**0.0038**	**0.034**	**0.342**	0.252	**0.024**	**0.038**	0.039	**0.0003**	**0.061**
	ppn		-0.60	-0.0030	-0.022	0.011	0.003	-0.099	-0.0026	-0.016	0.235	0.056	**0.018**	0.014	0.061	-0.0004	-0.004
	lu		**-0.97**	**-0.0002**	**0.013**	**-0.006**	**-0.001**	**-0.062**	**0.0037**	**0.019**	**-0.572**	0.044	**0.005**	**0.022**	0.004	0.0000	0.035
	Ndep		**0.16**	**-0.0002**	0.000	**-0.007**	**0.000**	**0.048**	-0.0002	**0.023**	**0.144**	**0.316**	**0.002**	**0.017**	**0.024**	**0.0004**	0.035
	pop		**-0.91**	**-0.0003**	**-0.009**	**-0.016**	**-0.001**	0.022	**-0.0020**	**-0.027**	**-0.312**	-0.076	**-0.002**	0.009	**0.041**	0.0001	0.036
	CO2		0.02	-0.0001	0.004	**-0.006**	**-0.004**	-0.001	**0.0007**	**0.036**	**0.245**	0.081	**0.003**	0.027	**0.025**	**0.0002**	**0.046**
	HDI		**-4.45**	**-0.0211**	-0.054	-0.044	-0.009	-0.335	-0.0123	-0.111	-0.806	-1.471	-0.121	-0.236	-0.205	-0.0006	-0.181

burnt area trends for CEAM, NHSA, BOAS and CEAS. For MIDE, precipitation has a dominant role in reducing burnt area. On the other hand, despite dominating the burnt area trends, temperature and precipitation can have opposite effects. Namely, for BONA (not significant for air temperature), TENA , SHSA, EURO , and AUST, precipitation causes a reduction in burnt

285   area, while temperature results in an increase, although results are not statistically significant for precipitation over TENA, SHSA, EURO, CEAS, CEAM and AUST.

Anthropogenic drivers, such as land use and population density can play a major role in some regions. For example, land use is the dominant driver in SHSA and SHAF, population density in CEAM, and both drivers in TENA, EURO, MIDE, NHAF. Land use can have cause either an increase (TENA, EURO, and SHAF) or a decrease in burnt area, while population density

290   results in a reduction in burnt area for all the regions where this external driver is dominant (TENA, CEAM, EURO, MIDE, and NHAF).

Biogenic drivers such as nitrogen deposition and atmospheric carbon dioxide tend to play a less significant role in the burnt area trends, impacting burnt area trends only for NHSA through carbon dioxide, and CEAS through both nitrogen deposition and atmospheric carbon dioxide.

295   As seen before, HDI is the dominant driver in the burnt area trend for all regions, with the exception of NHAF and EQAS. This is evident in the sensitivity experiments for JULES-INFERNO+HDI where only HDI forcing is made transient (**HDI**). In all cases, including socio-economic factors in INFERNO changes the relative role that external forcings have in determining burnt area trends. For example, it reduces the role that climate, population density, and land use have in burnt area trends towards a stronger role from socio-economic effects (HDI).

300   This impact is especially evident when comparing the role of the climate forcing in driving burnt area trends between JULES-INFERNO and JULES-INFERNO+HDI in their respective sensitivity experiments, *clim*, *tas*, and *ppn*. For instance, where temperature effects on burnt area trends were dominant in JULES-INFERNO, they show less of an impact on the burnt area trends in JULES-INFERNO+HDI, but still statistically significant (e.g., TENA, EURO, CEAS, and AUS). In addition, where the climate contributions to the burnt area trends were small in JULES-INFERNO (BONA, CEAM, and NHSA), when

305   considering socio-economic factors, these become statistically non-significant in terms of the climate contributions to the trends. In addition, including socio-economic factors in INFERNO led to a change in how precipitation and temperature can impact some regions. For example, for MIDE, in JULES-INFERNO precipitation was the dominant driver of burnt area trends, causing a reduction of burnt area in this region (trend of -0.038 $Mha\,year^{-1}$). Conversely, in JULES-INFERNO+HDI, precipitation has less impact on the burnt area trend ((trend of -0.016 $Mha\,year^{-1}$), while temperature has a larger impact on

310   the burnt area trend (+0.034 $Mha\,year^{-1}$). A similar result is also seen for NHAF, where the role of temperature becomes statistically significant in JULES-INFERNO+HDI (trend of +0.342 $Mha\,year^{-1}$), while it was not statistically significant in JULES-INFERNO (trend of +0.007 $Mha\,year^{-1}$).

Moreover, results also show an impact on the role of anthropogenic drivers (land use and population density) on burnt area trends between JULES-INFERNO and JULES-INFERNO+HDI sensitivity experiments. For BONA, CEAM, and NHSA re-

315   gions, burnt area decreases for JULES-INFERNO+HDI (*pop* and *lu*) sensitivity experiments while for JULES-INFERNO+HDI (*pop* and *lu*) an increase was observed.

15

Together, these results show that including socio-economic factors in the representation of fires in Earth System Models is important for realistically simulating the burnt area mean state, for quantifying burnt area trends and for understanding the main drivers of those trends at regional scales.

4 Conclusions

Discussion & Conclusions This work aimed to represent socio-economic factors, through the use of the HDI, together with the Pechony and Shindell (2009) anthropogenic fire ignitions to parameterise human socio-economic impacts on fires. When using the INFERNO fire model, the aim was to improve the regional representation of human–environmental coupling for applications at large spatial scales within an ESM.

The results presented in this study show that including socio-economic factors in the fire ignition and suppression parametrisation within INFERNO leads to improved performance in regions that were affected by large biases in the JULES-INFERNO configuration, without having a negative impact in regions that perform well when compared to GFED4s. Large bias reductions are evident in TENA, CEAM, SHSA, EURO and MIDE, with the largest reductions in TENA where a 735.57 % bias in JULES-INFERNO is reduced to 44.46 % in JULES-INFERNO+HDI. Furthermore, it should be highlighted that although JULES-INFERNO performs well at the global scale, as can be seen when comparing the annual mean burnt area against GFED4s in Table 2, this is due to compensating errors at the regional level.

Moreover, including socio-economic factors in INFERNO-JULES+HDI improves the representation of the burnt area trends, especially in areas where GFED4s presents negative trends. At the same time, JULES-INFERNO shows no significant trends (e.g., SHSA, NHAF, CEAS, and AUST), as well as better representing regions with weak negative burnt are trends (CEAM, NHSA, EURO, and BOAS). However, JULES-INFERNO+HDI can also produce too strong trends (e.g., SHAF) or misrepresents the observed positive burnt area trends found in TENA, MIDE and SEAS.

Overall, the improved representation of the burnt area trends in JULES-INFERNO+HDI when compared to JULES-INFERNO highlights the importance of including the socio-economic factors in fire ignitions and suppression in order to confidently reproduces the observed fire trends. This impact is especially evident when comparing the role of external climate drivers on burnt area trends between JULES-INFERNO and JULES-INFERNO+HDI using a set of sensitivity experiments. The results of these experimeents have shown that including the socio-economic impacts on fire results in the burnt areas trends being dominated by the socio-economic drivers, through a reduction in the contribution from climate drivers, especially from temperature and precipitation.

4.1 Modelled burnt area trends

We show that introducing the representation of socio-economic factors can change the impact external forcing has on burnt area trends and that the mechanisms that lead to this can differ at a regional level. For example, the inclusion of socio-economic factors reduce the role of temperature in driving trends by reducing the role of temperature in driving trends (e.g., increase for TENA, EURO, CEAS, and AUS), as well as by changing the behaviour of climate drivers have in burnt area trends (e.g.,

MIDE, NHAF, and SEAS). Socio-economic effects on fire also change the role of land use and population by changing the

350 role land use and population density towards more impact through the socio-economic fire effects (e.g., BONA, CEAM, and NHSA).

These results are consistent with other studies, which show that for developed regions, land and fire management policies have a greater role than other human behaviours in controlling ignitions (Nikolakis and Roberts, 2022; Ford et al., 2021; Jacobson et al., 2022; Carreiras et al., 2014; Mourão and Martinho, 2014).

355 The work of Kelley et al. (2019) and Jones et al. (2022) shows that, despite the increases in fire weather seasons and fire weather extremes that have been observed in all world regions, burnt area has shown a variety of regional trends and that the negative trends were found to be significant only in Africa (NHAF and SHAF), Europe (EURO), and Central Asia (CEAS). At a global scale, burnt area trends show a decline predominantly driven by a decline in burnt area in the savannah-grassland systems caused by the expansion of high-capital agriculture (Andela et al., 2017), as well as reductions in vegetation productivity driven

360 by changes to the hydrological balance (Zubkova et al., 2019). The results on the impact of external model drivers on burnt area trends, detailed in Section 3.2.1, agree with this. In both JULES-INFERNO and JULES-INFERNO+HDI, the dominant forcings contributing to the negative trend in global burnt area are linked to anthropogenic drivers (land use, population density and HDI), as well as precipitation. Several authors have also shown that declines in burnt area in the Mediterranean have occurred irrespective of increases in fire weather, as well as extensions to the fire weather season length, which is attributed to

365 increased fire prevention and in combating and mitigating fire impacts (Jones et al., 2022; Urbieta et al., 2019; Carreiras et al., 2014; Mourão and Martinho, 2014).

Moreover, results also show an impact on the anthropogenic drivers (land use and population density) in the burnt area trends, resulting in a decrease in burnt area for JULES-INFERNO+HDI compared to JULES-INFERNO, for BONA, CEAM, and NHSA regions. This result, combined with the impact seen in the reduction of the effects temperature has in burnt area,

370 are especially relevant in South America (NHSA and SHSA), leading to a better performance of JULES-INFERNO+HDI in these regions overall. The impact of socio-economic effects on fire is also documented for the Amazonia region, where fire is routinely used for land clearing, resulting in a strong link between burnt area and deforestation rates. Through the last decade, this region has seen a decline in deforestation rates leading to an observed negative trend in burnt area. However, this decline in burnt area has not been uniform due to historical shifts in economic and environmental policies (Silva Junior et al., 2021;

375 Aragão et al., 2018; Nepstad et al., 2014).

The analysis of the impact of including socio-economic factors in INFERNO has also shown that JULES-INFERNO+HDI can also produce trends that are too strong, leading to too strong negative trends resulting in worse performance when compared to JULES-INFERNO (e.g., SHAF). In addition, for regions where observations present a positive burnt area trend (TENA, MIDE and SEAS) JULES-INFERNO+HDI presents an opposite trend sign (negative), while JULES-INFERNO is able to

380 capture the positive trend in TENA and SEAS.

It is known that there is an increases in the frequency of large and severe fires in Continental United States of America (Goss et al., 2020; Williams et al., 2019; Abatzoglou and Williams, 2016), as well as boreal regions (Canada and Alaska) (Kasischke and Turetsky, 2006; Stocks et al., 2002; Veraverbeke et al., 2017), leading to observed increases in burnt area, with fire activity

having a strong relationship with fire weather in these regions. However, due to the nature of model resolutions and timescales

385   in Earth System Modelling, INFERNO was not designed to model the processes that are needed to represent large and severe fires which dominate the trends and fire regime characteristics of these regions (e.g., it is based on the use of a value for the average burnt area for each plant functional type). Therefore, it is expected that regions where fire regimes are dominated by large and severe fires may be affected by a negative bias in burnt areas and fire emissions, as well as on their response to a changing climate.

390   **4.2   Model limitations and known issues**

The use of socio-economic factors in INFERNO reduces the inter-annual variability of burnt area for most of the fire regions (Figure 5). While this benefits INFERNO performance over regions such as TENA and CEAM, it results in a reduction in the variability overall, reducing the ability of the model to represent the burnt area regions that are characterised by high inter-annual variability, namely, BONA, BOAS, AUST, CEAS, SHSA and NHSA. Although this is seen as a negative impact, it

395   must be noted that the control model - JULES-INFERNO - despite having a larger inter-annual variability, also has a poor performance in this aspect compared to observations.

Although socio-economic factors are included in JULES-INFERNO+HDI, the HDI dataset provides information mainly at a national level. To improve the impact of socioeconomic activities on fire at a regional level, it would be beneficial to use data capturing the HDI changes at a sub-national administrative level. Furthermore, it should be highlighted that the HDI does not

400   account for the different implementation of fire management practices and government policies at the regional level.

It should also be highlighted that INFERNO does not include a peat-burning capability. The work of Teixeira et al. (2021) highlights that this could be responsible for the negative bias over equatorial Asia and boreal regions where peatland fires represent a significant amount of burnt area and biomass burning emissions. Further work in this area could significantly improve the model performance over these regions and help to reduce the burnt area bias both at regional and global scales.

405   In addition, and as shown by Teixeira et al. (2021), biases in the underlying vegetation can significantly impact on the modelled burnt area. Despite the improvements introduced by Burton et al. (2019b) to JULES, including fire-vegetation interactions, there are still a number of regions that present significant vegetation biases, which in turn affect the performance of INFERNO. For example, it is known that JULES vegetation has few needle-leaf trees across the boreal regions compared to observations. Moreover, the trees across the extratropics and savanna regions are notably reduced.

410   These results highlight that the high burnt area variability in these regions may result from a mechanism not currently represented in INFERNO. For example, Kirillina et al. (2020); Andela and Van Der Werf (2014) show how changes in areas with increasing anthropogenic alteration, such as agricultural systems, and changes in fire management practices and government policies, often lead to shifts in peak fire activity for regions such as India and southwest Russia. They also show that the widespread adoption of Aboriginal fire management with increased prescribed burning has curbed the frequency of large fires

415   over a broad region in Australia. Similarly, the dominant spatial and temporal variability in the burnt area for Southern Europe and North Africa (Chergui et al., 2018), as well as South America (Chuvieco et al., 2021), is known to be driven by shifts in the amounts of fuel and continuity imposed by changes in socioeconomic drivers.

18

4.3 Concluding remarks

This study shows that including a parametrisation for socio-economic impacts on fire based on HDI in INFERNO provides
420 a simple and linear representation of these effects on fire ignition and suppression. This leads to an improvement in model performance, especially in developed regions.

Furthermore, several authors have shown that socio-economic policies on management and control of fire play a major role in controlling fire ignition and suppression (Nikolakis and Roberts, 2022; Ford et al., 2021; Jacobson et al., 2022; Carreiras et al., 2014; Mourão and Martinho, 2014). This is especially important in the context of future climate projections (Pivello
425 et al., 2021; Duane et al., 2019; Gillson et al., 2019; Paveglio et al., 2018). It is only with the understanding of the expected impact of climate change that adaptation and mitigation policies can be developed with the aim of protecting infrastructure and ecosystems from fire hazards. This shows the importance of representing socio-economic controls on fire when modelling future projections in the Earth System Modelling context.

Introducing socio-economic factors into INFERNO, reduces compensating biases and improves the modelled burnt area
430 trends in comparison with observations. In particular, the results here show that including socio-economic factors in the representation of fires in Earth System Models is important for realistically simulating the burnt area mean state, for quantifying burnt area trends in the recent past, and for understanding the main drivers of those trends at regional scales.

Considering this, we recommend that socio-economic factors should be included in all fire modelling studies at both global and regional scales, particularly when considering future climate change scenarios. This work will form the basis of a future
435 study on understanding the impact of fires in the Earth System when considering future climate change scenarios.
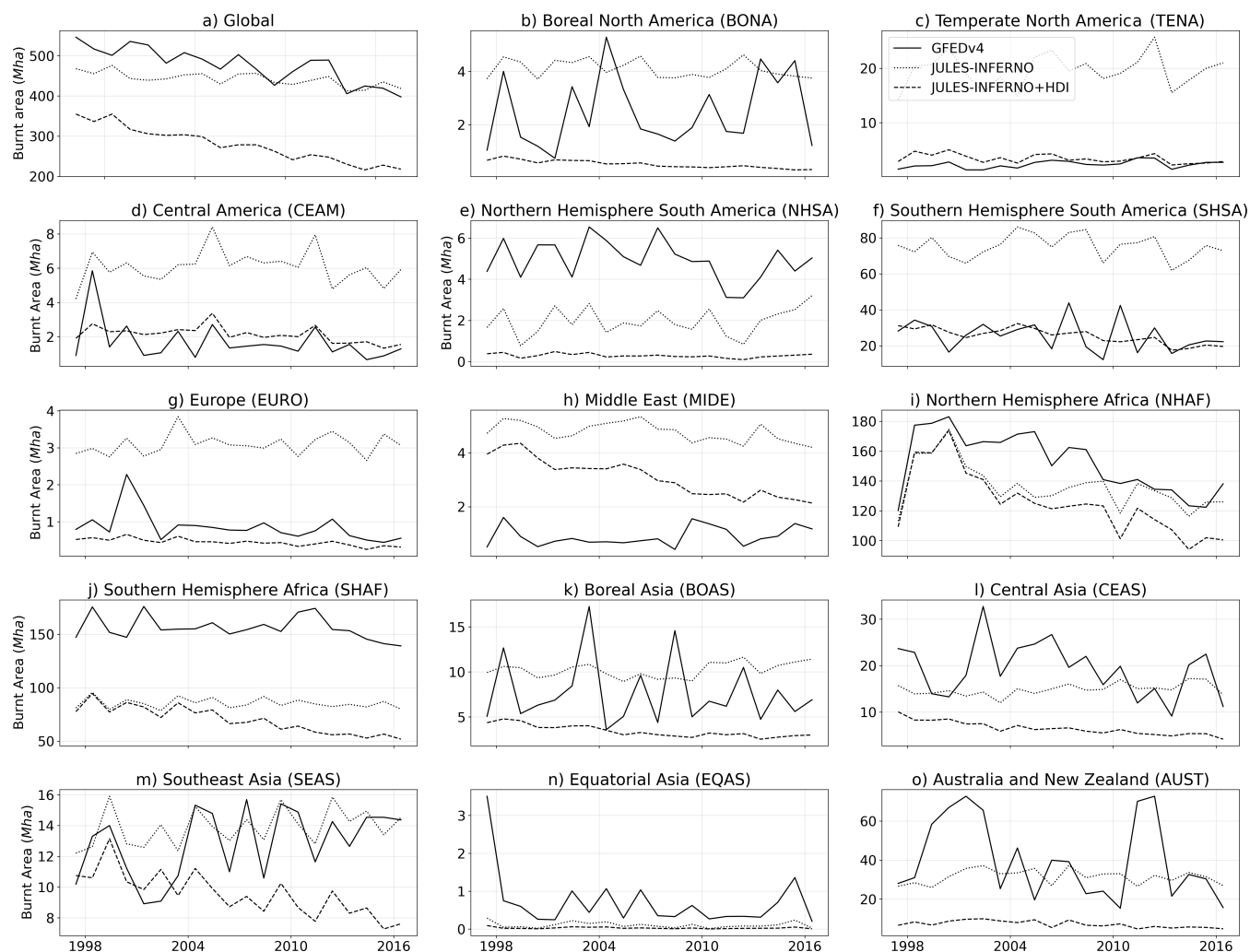
Appendix A

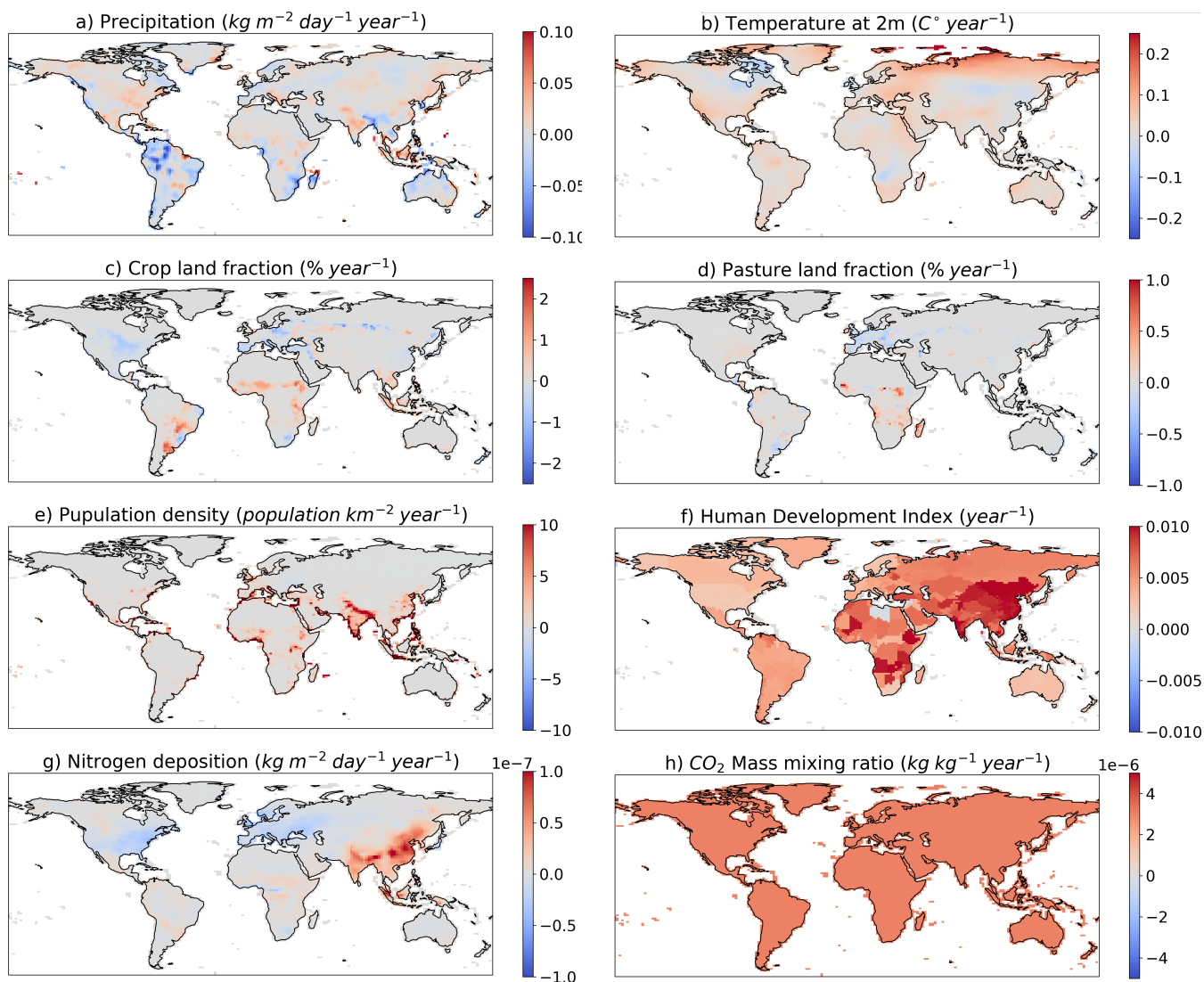**Figure A1.** Burnt area annual mean time series (Mha).

Figure A2. Trends calculated between the period 1997 - 2016 for JULES-ES external forcing variables a) Precipitation ($kg\ m^{-2}\ day^{-1}\ year^{-1}$), b) Temperature at 2 m ($C^{\circ}\ year^{-1}$), c) Crop land fraction ($\%\ year^{-1}$), d) Pasture land fraction ($\%\ year^{-1}$), e) Population density ($population\ km^{-2}\ year^{-1}$), f) Human Development Index ($year^{-1}$), g) Nitrogen deposition ($kg\ m^{-2}\ day^{-1}\ year^{-1}$), and h) Carbon Dioxide mixing ration ($kg\ m^{-2}\ day^{-1}\ year^{-1}$).

Biogeosciences
Discussions

EGU

Code and data availability. Both the model code and the files for running it are available from the Met Office Science Repository Service: https://code.metoffice.gov.uk/ (last access: 26 July 2023). Registration is required, and code is freely available subject to completion of a software license.

440   Details of the simulations performed: JULES simulations are compiled and run in suites developed using the Rose suite engine (MetOffice, 2022) and scheduled using the cylc workflow engine (Oliver et al., 2019). Both Rose and cylc are available under v3 of the GNU General Public License (GPL). In this framework, the suite contains the information required to extract and build the code as well as configure and run the simulations. Each suite is labelled with a unique identifier and is held in the same revision-controlled repository service in which we hold and develop the model code. This means that these suites are available to any licensed of JULES under the following suite IDs:

445   – JULES-INFERNO: u-by849

    – JULES-INFERNO+HDI: u-by851

    For JULES-INFERNO sensitivity experiments:

    – 1990 control: u-co594

    – clim: u-cs067

450   – tas: u-cs068

    – ppn: u-cs069

    – lu: u-cr440

    – Ndep: u-cr441

    – pop: u-cr442

455   – CO_2: u-cr443

    For JULES-INFERNO+HDI sensitivity experiments:

    – 1990 control: u-ct759

    – clim: u-cs070

    – tas: u-cs071

460   – ppn: u-cs072

    – lu: u-cr447

    – Ndep: u-cr448

    – pop: u-cr449

    – CO_2: u-cr450

465   – HDI: u-cn957

Author contributions. JCMT led the writing of the paper and model development. All co-authors contributed to the simulation design, writing sections, performing evaluation and reviewing drafts of the paper.

Biogeosciences
Discussions

References

Abatzoglou, J. T. and Williams, A. P.: Impact of anthropogenic climate change on wildfire across western US forests, Proceedings of the National Academy of Sciences, 113, 11 770–11 775, 2016.

480 Andela, N. and Van Der Werf, G. R.: Recent trends in African fires driven by cropland expansion and El Nino to La Nina transition, Nature Climate Change, 4, 791–795, 2014.

Andela, N., Morton, D. C., Giglio, L., Chen, Y., van der Werf, G. R., Kasibhatla, P. S., DeFries, R. S., Collatz, G., Hantson, S., Kloster, S., et al.: A human-driven decline in global burned area, Science, 356, 1356–1362, 2017.

Andela, N., Morton, D. C., Giglio, L., Paugam, R., Chen, Y., Hantson, S., Van Der Werf, G. R., and Randerson, J. T.: The Global Fire Atlas
485 of individual fire size, duration, speed and direction, Earth System Science Data, 11, 529–552, 2019.

Aragão, L. E., Anderson, L. O., Fonseca, M. G., Rosan, T. M., Vedovato, L. B., Wagner, F. H., Silva, C. V., Silva Junior, C. H., Arai, E., Aguiar, A. P., et al.: 21st Century drought-related fires counteract the decline of Amazon deforestation carbon emissions, Nature communications, 9, 536, 2018.

Archibald, S., Roy, D. P., van Wilgen, B. W., and Scholes, R. J.: What limits fire? An examination of drivers of burnt area in Southern Africa,
490 Global Change Biology, 15, 613–630, 2009.

Best, M. J., Pryor, M., Clark, D. B., Rooney, G. G., Essery, R. L. H., Ménard, C. B., Edwards, J. M., Hendry, M. A., Porson, A., Gedney, N., Mercado, L. M., Sitch, S., Blyth, E., Boucher, O., Cox, P. M., Grimmond, C. S. B., and Harding, R. J.: The Joint UK Land Environment Simulator (JULES), model description – Part 1: Energy and water fluxes, Geoscientific Model Development, 4, 677–699, https://doi.org/10.5194/gmd-4-677-2011, 2011.

495 Bhanojirao, V.: Human development report 1990: review and assessment, World Development, 19, 1451–1460, 1991.

Bowman, D. M., Balch, J. K., Artaxo, P., Bond, W. J., Carlson, J. M., Cochrane, M. A., D'Antonio, C. M., DeFries, R. S., Doyle, J. C., Harrison, S. P., et al.: Fire in the Earth system, science, 324, 481–484, 2009.

Bowman, D. M., Balch, J., Artaxo, P., Bond, W. J., Cochrane, M. A., D'antonio, C. M., DeFries, R., Johnston, F. H., Keeley, J. E., Krawchuk, M. A., et al.: The human dimension of fire regimes on Earth, Journal of biogeography, 38, 2223–2236, 2011.

500 Bowman, D. M., Kolden, C. A., Abatzoglou, J. T., Johnston, F. H., van der Werf, G. R., and Flannigan, M.: Vegetation fires in the Anthropocene, Nature Reviews Earth & Environment, 1, 500–515, 2020.

Burton, C., Betts, R., Cardoso, M., Feldpausch, T. R., Harper, A., Jones, C. D., Kelley, D. I., Robertson, E., and Wiltshire, A.: Representation of fire, land-use change and vegetation dynamics in the Joint UK Land Environment Simulator vn4.9 (JULES), Geoscientific Model Development, 12, 179–193, https://doi.org/10.5194/gmd-12-179-2019, 2019a.

505 Burton, C., Betts, R., Cardoso, M., Feldpausch, T. R., Harper, A., Jones, C. D., Kelley, D. I., Robertson, E., and Wiltshire, A.: Representation of fire, land-use change and vegetation dynamics in the Joint UK Land Environment Simulator vn4. 9 (JULES), Geoscientific Model Development, 12, 179–193, 2019b.

Burton, C., Betts, R. A., Jones, C. D., Feldpausch, T. R., Cardoso, M., and Anderson, L. O.: El Niño Driven Changes in Global Fire 2015/16, Frontiers in Earth Science, 8, 199, https://doi.org/10.3389/feart.2020.00199, 2020.

510 Carreiras, M., Ferreira, A. J. D., Valente, S., Fleskens, L., Gonzales-Pelayo, Ó., Rubio, J. L., Stoof, C. R., Coelho, C. O. A., Ferreira, C. S. S., and Ritsema, C. J.: Comparative analysis of policies to deal with wildfire risk, Land Degradation & Development, 25, 92–103, 2014.

Cecil, D.: LIS/OTD 0.5 Degree High Resolution Monthly Climatology (HRMC), https://doi.org/10.3389/feart.2020.00199, 2006.

Biogeosciences
Discussions

Chergui, B., Fahd, S., Santos, X., and Pausas, J. G.: Socioeconomic factors drive fire-regime variability in the Mediterranean Basin, Ecosystems, 21, 619–628, 2018.

515 Chinamatira, L., Mtetwa, S., and Nyamadzawo, G.: Causes of wildland fires, associated socio-economic impacts and challenges with policing, in chakari resettlement area, kadoma, zimbabwe, Fire Science Reviews, 5, 1, 2016.

Chuvieco, E., Pettinari, M. L., Koutsias, N., Forkel, M., Hantson, S., and Turco, M.: Human and climate drivers of global biomass burning variability, Science of the Total Environment, 779, 146 361, 2021.

Clark, D. B., Mercado, L. M., Sitch, S., Jones, C. D., Gedney, N., Best, M. J., Pryor, M., Rooney, G. G., Essery, R. L. H., Blyth, E., Boucher,
520 O., Harding, R. J., Huntingford, C., and Cox, P. M.: The Joint UK Land Environment Simulator (JULES), model description – Part 2: Carbon fluxes and vegetation dynamics, Geoscientific Model Development, 4, 701–722, https://doi.org/10.5194/gmd-4-701-2011, 2011.

Cox, P.: Description of the "TRIFFID" Dynamic Global Vegetation Mode, 2001.

Cox, P., Betts, R., Jones, C., Spall, S., and Totterdell, I.: Acceleration of global warming due to carbon-cycle feedbacks in a coupled climate model, Nature, 408, 184–187, 2000.

525 Daniau, A.-L., Goñi, M. F. S., Martinez, P., Urrego, D. H., Bout-Roumazeilles, V., Desprat, S., and Marlon, J. R.: Orbital-scale climate forcing of grassland burning in southern Africa, Proceedings of the National Academy of Sciences, 110, 5069–5073, 2013.

Duane, A., Aquilué, N., Canelles, Q., Morán-Ordóñez, A., De Cáceres, M., and Brotons, L.: Adapting prescribed burns to future climate change in Mediterranean landscapes, Science of the Total Environment, 677, 68–83, 2019.

Ford, A. E., Harrison, S. P., Kountouris, Y., Millington, J. D., Mistry, J., Perkins, O., Rabin, S. S., Rein, G., Schreckenberg, K., Smith, C.,
530 et al.: Modelling human-fire interactions: combining alternative perspectives and approaches, Frontiers in Environmental Science, p. 418, 2021.

Giglio, L., Randerson, J. T., and Van Der Werf, G. R.: Analysis of daily, monthly, and annual burned area using the fourth-generation global fire emissions database (GFED4), Journal of Geophysical Research: Biogeosciences, 118, 317–328, 2013.

Gillson, L., Whitlock, C., and Humphrey, G.: Resilience and fire management in the Anthropocene, Ecology and Society, 24, 2019.

535 Goldewijk, K. K., Dekker, S. C., and van Zanden, J. L.: Per-capita estimations of long-term historical land use and the consequences for global change research, Journal of Land Use Science, 12, 313–337, https://doi.org/10.1080/1747423X.2017.1354938, 2017.

Goss, M., Swain, D. L., Abatzoglou, J. T., Sarhadi, A., Kolden, C. A., Williams, A. P., and Diffenbaugh, N. S.: Climate change is increasing the likelihood of extreme autumn wildfire conditions across California, Environmental Research Letters, 15, 094 016, 2020.

Harris, I., Jones, P. D., Osborn, T. J., and Lister, D. H.: Updated high-resolution grids of monthly climatic observations–the CRU TS3. 10
540 Dataset, International journal of climatology, 34, 623–642, 2014.

Jacobson, M., Smith, H., Huber-Stearns, H. R., Davis, E. J., Cheng, A. S., and Deak, A.: Comparing social constructions of wildfire risk across media, government, and participatory discourse in a Colorado fireshed, Journal of Risk Research, 25, 697–714, 2022.

Jones, M. W., Abatzoglou, J. T., Veraverbeke, S., Andela, N., Lasslop, G., Forkel, M., Smith, A. J., Burton, C., Betts, R. A., van der Werf, G. R., et al.: Global and regional trends and drivers of fire under climate change, Reviews of Geophysics, p. e2020RG000726, 2022.

545 Kasischke, E. S. and Turetsky, M. R.: Recent changes in the fire regime across the North American boreal region—Spatial and temporal patterns of burning across Canada and Alaska, Geophysical research letters, 33, 2006.

Kelley, D. I., Bistinas, I., Whitley, R., Burton, C., Marthews, T. R., and Dong, N.: How contemporary bioclimatic and human controls change global fire regimes, Nature Climate Change, 9, 690–696, 2019.

Biogeosciences
Discussions

Kirillina, K., Shvetsov, E. G., Protopopova, V. V., Thiesmeyer, L., and Yan, W.: Consideration of anthropogenic factors in boreal forest
    fire regime changes during rapid socio-economic development: case study of forestry districts with increasing burnt area in the Sakha
    Republic, Russia, Environmental Research Letters, 15, 035 009, 2020.

Klein Goldewijk, K., Beusen, A., Doelman, J., and Stehfest, E.: Anthropogenic land use estimates for the Holocene – HYDE 3.2, Earth
    System Science Data, 9, 927–953, https://doi.org/10.5194/essd-9-927-2017, 2017.

Kummu, M., Taka, M., and Guillaume, J. H.: Gridded global datasets for gross domestic product and Human Development Index over
    1990–2015, Scientific data, 5, 180 004, 2018.

Laris, P.: Burning the seasonal mosaic: preventative burning strategies in the wooded savanna of southern Mali, Human Ecology, 30, 155–186,
    2002.

Li, F., Levis, S., and Ward, D.: Quantifying the role of fire in the Earth system–Part 1: Improved global fire modeling in the Community
    Earth System Model (CESM1), Biogeosciences, 10, 2293–2314, 2013.

Mangeon, S., Voulgarakis, A., Gilham, R., Harper, A., Sitch, S., and Folberth, G.: INFERNO: a fire and emissions scheme for the UK Met
    Office's Unified Model, Geoscientific Model Development, 9, 2685–2700, 2016.

Marlon, J. R., Bartlein, P. J., Carcaillet, C., Gavin, D. G., Harrison, S. P., Higuera, P. E., Joos, F., Power, M., and Prentice, I.: Climate and
    human influences on global biomass burning over the past two millennia, Nature Geoscience, 1, 697–702, 2008.

Mathison, C., Burke, E., Hartley, A. J., Kelley, D. I., Burton, C., Robertson, E., Gedney, N., Williams, K., Wiltshire, A., Ellis, R. J., et al.:
    Description and Evaluation of the JULES-ES setup for ISIMIP2b, EGUsphere, 2022, 1–24, 2022.

MetOffice: Rose suite engine, https://metomi.github.io/rose/doc/html/index.html, 2022.

Mourão, P. R. and Martinho, V. D.: The choices of the fire—Debating socioeconomic determinants of the fires observed at Portuguese
    municipalities, Forest Policy and Economics, 43, 29–40, 2014.

Nepstad, D., McGrath, D., Stickler, C., Alencar, A., Azevedo, A., Swette, B., Bezerra, T., DiGiano, M., Shimada, J., Seroa da Motta, R.,
    et al.: Slowing Amazon deforestation through public policy and interventions in beef and soy supply chains, science, 344, 1118–1123,
    2014.

Nikolakis, W. and Roberts, E.: Wildfire governance in a changing world: Insights for policy learning and policy transfer, Risk, Hazards &
    Crisis in Public Policy, 13, 144–164, 2022.

Oliver, H., Shin, M., Matthews, D., Sanders, O., Bartholomew, S., Clark, A., Fitzpatrick, B., van Haren, R., Hut, R., and Drost, N.: Workflow
    automation for cycling systems, Computing in Science & Engineering, 21, 7–21, 2019.

Paveglio, T. B., Carroll, M. S., Stasiewicz, A. M., Williams, D. R., and Becker, D. R.: Incorporating social diversity into wildfire management:
    Proposing "pathways" for fire adaptation, Forest Science, 64, 515–532, 2018.

Pechony, O. and Shindell, D.: Fire parameterization on a global scale, Journal of Geophysical Research: Atmospheres, 114, 2009.

Pfeiffer, M., Spessa, A., and Kaplan, J. O.: A model for global biomass burning in preindustrial time: LPJ-LMfire (v1. 0), Geoscientific
    Model Development, 6, 643–685, 2013.

Pivello, V. R., Vieira, I., Christianini, A. V., Ribeiro, D. B., da Silva Menezes, L., Berlinck, C. N., Melo, F. P., Marengo, J. A., Tornquist,
    C. G., Tomas, W. M., et al.: Understanding Brazil's catastrophic fires: Causes, consequences and policy needed to prevent future tragedies,
    Perspectives in Ecology and Conservation, 19, 233–255, 2021.

Rabin, S. S., Melton, J. R., Lasslop, G., Bachelet, D., Forrest, M., Hantson, S., Kaplan, J. O., Li, F., Mangeon, S., Ward, D. S., et al.:
    The Fire Modeling Intercomparison Project (FireMIP), phase 1: experimental and analytical protocols with detailed model descriptions,
    Geoscientific Model Development, 10, 1175–1197, 2017.

Randerson, J., Chen, Y., Van Der Werf, G., Rogers, B., and Morton, D.: Global burned area and biomass burning emissions from small fires, Journal of Geophysical Research: Biogeosciences, 117, 2012.

Riley, K. L., Williams, A. P., Urbanski, S. P., Calkin, D. E., Short, K. C., and O'Connor, C. D.: Will landscape fire increase in the future? A

590   systems approach to climate, fire, fuel, and human drivers, Current Pollution Reports, 5, 9–24, 2019.

Sellar, A. A., Jones, C. G., Mulcahy, J. P., Tang, Y., Yool, A., Wiltshire, A., O'Connor, F. M., Stringer, M., Hill, R., Palmieri, J., Woodward, S., de Mora, L., Kuhlbrodt, T., Rumbold, S. T., Kelley, D. I., Ellis, R., Johnson, C. E., Walton, J., Abraham, N. L., Andrews, M. B., Andrews, T., Archibald, A. T., Berthou, S., Burke, E., Blockley, E., Carslaw, K., Dalvi, M., Edwards, J., Folberth, G. A., Gedney, N., Griffiths, P. T., Harper, A. B., Hendry, M. A., Hewitt, A. J., Johnson, B., Jones, A., Jones, C. D., Keeble, J., Liddicoat, S., Morgenstern,

595   O., Parker, R. J., Predoi, V., Robertson, E., Siahaan, A., Smith, R. S., Swaminathan, R., Woodhouse, M. T., Zeng, G., and Zerroukat, M.: UKESM1: Description and Evaluation of the U.K. Earth System Model, Journal of Advances in Modeling Earth Systems, 11, 4513–4558, https://doi.org/https://doi.org/10.1029/2019MS001739, 2019.

Silva Junior, C. H., Pessôa, A. C., Carvalho, N. S., Reis, J. B., Anderson, L. O., and Aragão, L. E.: The Brazilian Amazon deforestation rate in 2020 is the greatest of the decade, Nature Ecology & Evolution, 5, 144–145, 2021.

600   Solomon, S., Dube, K., Stone, K., Yu, P., Kinnison, D., Toon, O. B., Strahan, S. E., Rosenlof, K. H., Portmann, R., Davis, S., et al.: On the stratospheric chemistry of midlatitude wildfire smoke, Proceedings of the National Academy of Sciences, 119, e2117325 119, 2022.

Stocks, B., Mason, J., Todd, J., Bosch, E., Wotton, B., Amiro, B., Flannigan, M., Hirsch, K., Logan, K., Martell, D., et al.: Large forest fires in Canada, 1959–1997, Journal of Geophysical Research: Atmospheres, 107, FFR–5, 2002.

Sullivan, A., Kurvits, T., and E., B.: Spreading like Wildfire – The Rising Threat of Extraordinary Landscape Fires., United Nations Envi-

605   ronment Programme (UNEP), 2022.

Teckentrup, L., Harrison, S. P., Hantson, S., Heil, A., Melton, J. R., Forrest, M., Li, F., Yue, C., Arneth, A., Hickler, T., et al.: Response of sim- ulated burned area to historical changes in environmental and anthropogenic factors: a comparison of seven fire models, Biogeosciences, 16, 3883–3910, 2019.

Teixeira, J. C., Folberth, G. A., O'Connor, F. M., Unger, N., and Voulgarakis, A.: Coupling interactive fire with atmospheric composition and

610   climate in the UK Earth System Model, Geoscientific Model Development, 14, 6515–6539, 2021.

Urbieta, I. R., Franquesa, M., Viedma, O., and Moreno, J. M.: Fire activity and burned forest lands decreased during the last three decades in Spain, Annals of Forest Science, 76, 1–13, 2019.

Veraverbeke, S., Rogers, B. M., Goulden, M. L., Jandt, R. R., Miller, C. E., Wiggins, E. B., and Randerson, J. T.: Lightning as a major driver of recent large fire years in North American boreal forests, Nature Climate Change, 7, 529–534, 2017.

615   Viovy, N.: CRUNCEP version 7-atmospheric forcing data for the community land model, Research Data Archive at the National Center for Atmospheric Research, Computational and Information Systems Laboratory, 10, 2018.

Williams, A. P., Abatzoglou, J. T., Gershunov, A., Guzman-Morales, J., Bishop, D. A., Balch, J. K., and Lettenmaier, D. P.: Observed impacts of anthropogenic climate change on wildfire in California, Earth's Future, 7, 892–910, 2019.

Zubkova, M., Boschetti, L., Abatzoglou, J. T., and Giglio, L.: Changes in fire activity in Africa from 2002 to 2016 and their potential drivers,

620   Geophysical research letters, 46, 7643–7653, 2019.